AIAA JOURNAL
Vol. 44, No. 7, July 2006

Spanwise Characteristics of High-Aspect-Ratio Synthetic Jets

S. Abdou* and S. Ziada†
McMaster University, Hamilton, Ontario L8S 4L7, Canada

The spanwise characteristics, that is, the two dimensionality of two high-aspect-ratio, planar synthetic jets are investigated experimentally to evaluate their use as actuators for active flow control applications. The two jets, with different slit lengths, are generated through narrow axial slits on a cylinder by acoustical excitation at the cylinder terminations. Measurements of the mean and fluctuating velocities, as well as the phase of velocity fluctuations with respect to the excitation signal, are performed to study the effect of excitation frequency and amplitude on the steady and unsteady spanwise characteristics of the generated synthetic jet. The jet issuing from the long slit is found to exhibit large variations in the spanwise direction, in both its mean velocity and phase. These variations are also dependent on the level and frequency of acoustic excitation. For the short slit, the spanwise variations are substantially smaller. The test results indicate that the short slit is a favorable actuator for active control applications involving the generation of a planar synthetic jet with small spanwise variations. The long slit, however, may be useful for active control applications that require the inducement of large phase variations along the slit.

Nomenclature

D_i = inner-cylinder diameter
D_o = outer-cylinder diameter
d = height of the jet producing slit
f = frequency of synthetic jet driving mechanism
h = width of jet producing slit (orifice diameter in case of axisymmetric jet)
L = length of cylinder
L_o = synthetic jet stroke length
l = length of jet producing slit
Re_{Uo} = Reynolds number based on U_o
Sr = Strouhal number
U = mean streamwise velocity of the jet
U_c = mean centerline velocity of the jet
U_o = downstream-directed average exit nozzle velocity of synthetic jet $L_o f$
U' = normalized streamwise velocity of the jet, U/U_c
u_f = rms value of the streamwise velocity fluctuation at the fundamental frequency
u_{fc} = rms value of the streamwise velocity fluctuation at the fundamental frequency at the jet centerline
u'_f = normalized rms value of the streamwise velocity fluctuation at the fundamental frequency u_f/U_c
u_t = total rms value of the streamwise velocity fluctuation
u_{tc} = total rms value of the streamwise velocity fluctuation at the jet centerline
u'_t = normalized total rms value of the streamwise velocity fluctuation u_t/U_c
X = streamwise position of the hotwire
Y = cross-stream position of the hotwire
Z = spanwise position of the hotwire
$\Delta\theta$ = centerline phase difference between any spanwise position and slit midspan $\varphi_c - \varphi_{cm}$
$\Delta\varphi$ = phase difference between any cross-stream position and jet centerline, $\varphi - \varphi_c$
λ = wavelength of the waves produced by the driving mechanism, c/f
φ = phase of velocity fluctuations with respect to the jet excitation signal
φ_c = phase of velocity fluctuations with respect to the jet excitation signal at the jet centerline
φ_{cm} = centerline phase of velocity fluctuations with respect to the excitation signal at the slit midspan

Presented as Paper 2004-2855 at the AIAA/CEAS 10th Aeroacoustics Conference, Manchester, England, United Kingdom, 10–12 May 2004; received 31 August 2004; revision received 5 December 2005; accepted for publication 12 December 2005.

*Ph.D. Student, Department of Mechanical Engineering, 1280 Main Street West. Member AIAA.
†Professor, Department of Mechanical Engineering, 1280 Main Street West.

I. Introduction

THE concept of synthetic jets probably dates back to as early as 1950. At that time, however, the idea was merely used to study the circulation effects and the impedance of orifices where the formation of zero-net-mass-flux jets was observed.[1] The first use of synthetic jets as flow manipulation devices, however, was not until 1994 (Refs. 2 and 3).

A synthetic jet is a mean fluid motion created by intermittent suction and blowing through an orifice or a slit. The device that produces the jet usually consists of a neck driven by a pulsating diaphragm in a cavity, as shown in Fig. 1. Flow enters and exits the cavity through the orifice. During the intake stroke, fluid is drawn into the cavity from the fluid surrounding the orifice. As this fluid is driven out of the cavity, a shear layer is formed that rolls up to form a vortex ring, or a vortex pair in case of a two-dimensional slot. This vortex ring, or pair, convects downstream due to its induced velocity. By the time the diaphragm starts another intake stroke, the vortex ring has gained enough momentum and moved far enough away that it is virtually unaffected. Thus, a train of vortex rings is created by the actuator. In the mean, the velocity profile appears similar to a steady jet. The driver, or the diaphragm, of synthetic jets can take a number of different forms including acoustic drivers,[1,3–9] piezoelectric diaphragms,[10–17] and electromagnetically driven pistons.[18,19]

Synthetic jets possess a unique feature, that is, they are formed totally from the working fluid of the flow they are used in and, hence, require no external piping systems, making them a compact and low-cost system. This feature enables the synthetic jet also to transfer linear momentum to the flow without any net mass injection. This unique property and the fact that synthetic jets can exist in many different scales make the applications of synthetic jet numerous, especially in the area of flow manipulation and control. The uses of synthetic jets cover a wide range of applications including active flow control,[3,5,9,20–22] separation control,[6,13,23,24] virtual aeroshaping effects,[25–28] jet vectoring,[10,29,30] cooling,[31,32] and mixing enhancement.[32–35]

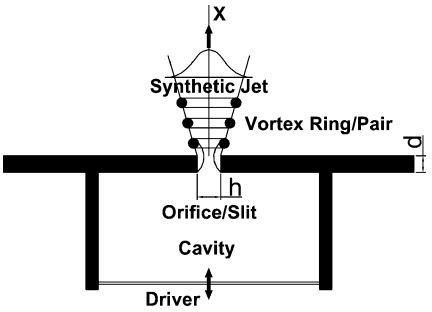

Fig. 1 Schematic of synthetic jet actuator.

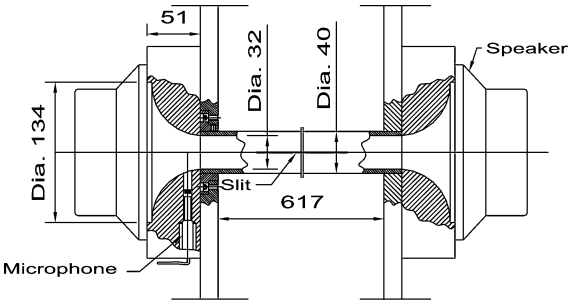

Fig. 2 Construction of apparatus generating the synthetic jet.

Since their first application in 1994 for flow manipulation, considerable research has been done to characterize synthetic jets and study their behavior both experimentally[6,7,10,11,20,30,35] as well as numerically.[14–18] Several excellent studies have been published discussing the characterization of synthetic jets covering different geometries, slit sizes, actuators and operating conditions. The work of Smith and Glezer,[11] Smith and Swift,[7,8] and Utturkar et al.[14] and a review paper by Glezer and Amitay[35] provide outstanding comprehensive analysis and characterization of synthetic jets.

Smith and Glezer[11] discuss the formation and characteristics of a high-aspect-ratio, piezoelectrically driven, synthetic jet formed in air. Schlieren images of the evolution of the synthetic jet are provided, which show the formation, convection, and then breakup of the vortex pairs formed at the slit exit. Smith and Glezer introduce two primary dimensionless parameters characterizing the synthetic jet, namely, a dimensionless stroke length L_o/h and a Reynolds number based on the average orifice velocity, Re_{U_o}. They conclude that the synthetic jet is similar to conventional two-dimensional turbulent jets in that cross-stream distribution of the time-averaged jet velocity components and their corresponding rms fluctuations collapse when plotted in the usual similarity coordinates.

In more recent studies, Smith and Swift[7,8] compare synthetic jets to continuous and pulsed jets. They developed a jet formation criterion whereby a threshold stroke length (or pulsation amplitude) for the formation of the jet was introduced. Mean velocity profiles plotted in similarity coordinates show that all of the jets collapse, being continuous, pulsed, or synthetic. The variation of the time-averaged centerline velocity with the downstream distance shows that synthetic jets start with a mean velocity of zero at the jet exit that increases to a value very close to that of continuous jets before the start of the half-power-law decay, typical of planar jets. Note that, despite the wide range of Reynolds number and stroke length covered in the tests, the jet behavior is similar for all of the cases.

Utturkar et al.[14] investigated the formation parameters of synthetic jets in search for a jet formation criterion. In the study, the same stroke length and Reynolds number based on U_o are used. They concluded a formation criterion $1/Sr > K$, where the Strouhal number $Sr = fh/U_o$ and the constant K is approximately 2 for two-dimensional synthetic jets and 0.16 for axisymmetric ones. This criterion is in good agreement with that suggested by Smith and Swift[7,8] and with their own experimental results.

Although the literature provides excellent and comprehensive analyses of the downstream evolution of uniformly excited synthetic jets, to the authors' knowledge, no references are available that provide spanwise characteristics of high-aspect-ratio synthetic jets that are not excited uniformly along the span of the slit. Knowledge of such characteristics is essential for practical applications of flow control because it is not always possible to generate synthetic jets by uniform excitations. (Examples of such applications may be found in Refs. 9 and 22.) In Ref. 9, the motivating work for the current study, although controlling the vibrations of the downstream cylinder in a tandem cylinder arrangement was achieved using a synthetic jet actuator hosted in the upstream cylinder, the fluid mechanics governing the process were not understood.

The present work deals primarily with the spanwise characteristics of the synthetic jet actuator for use as an actuator in flow control applications. The main focus is on the spanwise phase and amplitude distributions of nonuniformly excited long-aspect-ratio synthetic jets.

II. Experimental Setup

The synthetic jets studied herein are formed in air through rectangular slits having a width of $h = 0.75$ mm and two different slit lengths, $l = 580$ and 208 mm. These two cases provide aspect ratios of $l/h = 773$ and 273, respectively. The slits were milled axially on the surface of a polished aluminum cylinder with an outer diameter of $D_o = 40$ mm, an inner diameter of $D_i = 32$ mm, and a length $L = 651$ mm. The construction of the test facility is shown in Fig. 2. The excitation necessary to produce the synthetic jet was provided acoustically using a pair of high-quality Rockford Fosgard (FNQ2405) speakers mounted on each side of the cylinder through adapters to match the diameter of the speaker diaphragm to the cylinder inner diameter. The speakers are nominally rated at 200-W peak power with an acceptable response at low frequencies, down to about 70 Hz. A two-channel, 400-W power amplifier-type RAMSA (WP-1200) was used to power the speakers in parallel. The response of the two speakers to different inputs was measured to ensure their matching. The phase difference between the responses of the two speakers was found to be within 2 deg, whereas the difference between the amplitude ratios of the speakers' response was within 2%.

Sound pressure level measurements were conducted using a GRAS type 40BP microphone, with an accuracy of ± 1 dB, mounted inside the speaker adapter on one side of the cylinder as shown in Fig. 2. The microphone was installed through a 7-mm-diam hole and located about 40 mm away from the speaker and at about 37 mm away from the centerline of the adapter.

Velocity measurements of the issuing jet were performed using a Dantec Socket-type single-hotwire probe mounted on a traversing mechanism. The hotwire probe was powered by a single channel Dantec bridge, type 55M01, with an overheat ratio of 1.8. The traversing mechanism used is a Valmex (NF90 series), three-axis, computer-controlled traversing mechanism, allowing measurements in the spanwise, streamwise, and transverse directions. The traversing mechanism is capable of moving in steps of 0.005 mm/step. This traversing step is less than 1% of the slit width.

III. Experimental Procedure

Experiments were carried out by exciting the speakers in phase with harmonic signals at different frequencies and amplitudes. The response of the issuing synthetic jet to different excitations was then measured. Excitations were supplied to the speakers from a signal generator through an amplifier. The measured hotwire signal of the issuing synthetic jet along with the excitation signal were then sent to a personal computer data acquisition system for analysis and storage. A schematic diagram of the layout of the different components of the experiment is shown in Fig. 3.

Three different frequencies of 80, 100, and 120 Hz were used to excite the speakers. This frequency range was chosen because, in another set of experiments,[9] the same synthetic jet was used to control the vortex shedding process that occurred at this range of frequency. The amplitude of the signal exciting the speakers was set

Table 1 SPL measurements inside cylinder cavity for different test cases

		SPL, dB	
Frequency, Hz	Amplitude, V	Short-slit case	Long-slit case
80	4	135	133
100	2	129	128
100	4	135	134
100	6	138	137
120	4	135	134

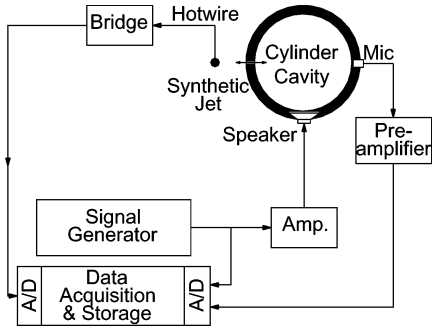

Fig. 3 Schematic of experimental setup and equipment used.

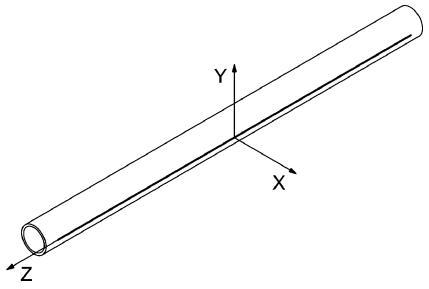

Fig. 4 Coordinate system used to describe hotwire location.

at 2, 4, and 6 V. These values include the gain of the amplifier. The case of 2 V was chosen because it represents the lowest amplitude that produced a measurable velocity signal at the midspan of the long-slit cylinder. Note, however, that these values of excitation were chosen based the vortex shedding control experiments that were performed using the current setup and configuration. The sound pressure levels (SPL) corresponding to these excitation values were measured inside the cylinder cavity and are given in Table 1. The sound pressure was measured by means of the microphone mounted in one of the speaker adapters as discussed earlier.

A system of axes was chosen to describe the position of the hotwire as shown in Fig. 4, the Z coordinate being in the spanwise direction along the cylinder axis, the Y coordinate being in the vertical or transverse direction, and the X coordinate being in the downstream direction. The origin of the axes is the midspan of the cylinder, the mid-width of the slit, and at the exit plane of the slit.

Nine spanwise measurement positions, in the Z direction, were chosen for each cylinder. For the long-slit cylinder, with an aspect ratio of $l/h = 773$, the positions were chosen as $Z/h = 0$, ± 77, ± 155, ± 232, and ± 309. In the short-slit case, with an aspect ratio of $l/h = 273$, the positions were $Z/h = 0$, ± 33, ± 67, ± 100, and ± 120. The streamwise position of the hotwire in the jet was fixed and was chosen to be at $X/h = 6.67$. At this location, traces of the suction stroke of the excitation cycle cease to exist in the hotwire signal as will be discussed later. Vertically, the hotwire was traversed across the centerline of the slit at each measurement position in steps of 0.25 mm. Steps of 0.125 mm were used near the centerline of the jet to ensure accurate measurement of the centerline velocity. The vertical traversing permitted obtaining the velocity profile at each location, as well as correcting slight misalignments between the axis of the traversing mechanism and the cylinder axis and, thereby, minimizing errors in estimating the centerline velocity or phase of the jet.

IV. Experimental Results

The following sections present the test results, starting with validating the characteristics of jet development. Thereafter, the spanwise distributions are given to show the effect of varying the excitation frequency and amplitude of the excitation signal on the spanwise characteristics of the synthetic jet.

A. Jet Characteristics

As mentioned earlier, this study focuses on the spanwise characteristics of high-aspect-ratio synthetic jets rather than on the downstream evolution of the jets. Although the latter issue has recently received considerable attention, as already discussed in the Introduction, measurements of the mean velocity profiles, as well as the phase and rms profiles, were performed for two reasons. First, it is necessary to validate that the investigated synthetic jet is similar to those investigated in the literature, and second, details of the jet are needed to determine the appropriate location (X and Y coordinates) for subsequent hotwire measurements to look at the spanwise distributions. It is also desirable to provide some typical characteristics of the investigated jet to allow comparisons with other synthetic jets reported in the literature.

Three downstream stations were investigated at $X/h = 0.67$, 6.67, and 13.33. Typical velocity traces measured at these three locations along the X axis, that is, $Y/h = Z/h = 0$, are shown in Fig. 5. Because of the inability of the hotwire anemometer to distinguish the direction of flow, the traces of the suction stroke near the jet exit are rectified as shown in Fig. 5a. Figures 5 also show that the mean velocity for the $X/h = 6.67$ position is higher than those at the other two locations. Smith and Swift[7,8] reported similar findings for all synthetic jet cases studied, where the average centerline velocity increases in the downstream direction until it reaches a maximum value near $X/h = 6$ before the start of typical turbulent jet decay. Based on these facts, it was decided to carry out the hotwire measurements at this location in the rest of the experiments.

Note that it was rather difficult and cumbersome to measure the velocity profiles at the exit of the slit, that is, at $X/h = 0$, to determine the values of L_o or U_o, and thereby characterize the jet at the exit. This difficulty was compounded by the fact that the jet characteristics vary along the span of the slit and are also functions of both the amplitude and frequency of actuation. When it was realized that it is not possible to describe the jet by a single Reynolds or Strouhal number, and that measuring L_o and U_o would be very cumbersome and would also obscure the main objective of the paper, which is to study the spanwise characteristics, the measurements at $X/h = 6.67$ were used to compare with the results in the literature. The profiles shown in Figs. 5–8 show similar trends to those reported in Refs. 7 and 8, where the behavior of the mean velocity was shown to be essentially the same regardless of the values of Reynolds number Re_{U_o}. In addition, the results given in Figs. 7 and 8 allow the comparison of the current jet with those presented in other references where the development of synthetic jets is discussed.

Figure 6 shows typical frequency spectra of the velocity signals shown in Fig. 5. Note in Fig. 6a that a higher first harmonic component of the fundamental frequency exists due to the rectified hotwire signal discussed earlier. For the other two spectra, the fundamental component is the strongest because of the diminishing effect of reverse flow. Figures 6b and 6c show increased broadband turbulence levels as reported in previous work.

For the chosen position of $X/h = 6.67$, characteristics of the produced jets at different spanwise measurement stations and for different frequencies and amplitudes of excitation were obtained. These characteristics include transverse profiles of mean velocity as well as the rms amplitude and phase difference of velocity fluctuations, all of which are plotted in similarity coordinates. Figures 7 and 8 show typical profiles obtained for the long and short slits, respectively. The profiles shown in Figs. 7 and 8 are obtained for an excitation frequency of 80 Hz and amplitude of 4 V. Measurements at other frequencies and amplitudes yielded similar trends, and therefore,

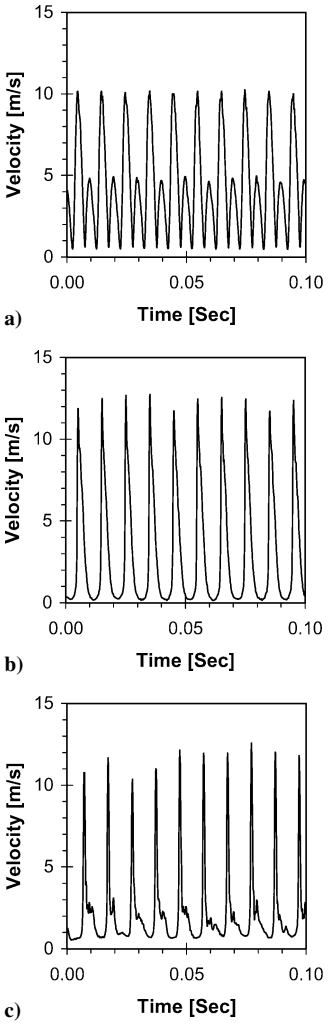

Fig. 5 Time traces of hotwire signal for long-slit cylinder at jet centerline at $Z/h = 0$ for excitation of 100 Hz and 4 V: a) $X/h = 0.67$, b) $X/h = 6.67$, and c) $X/h = 13.33$.

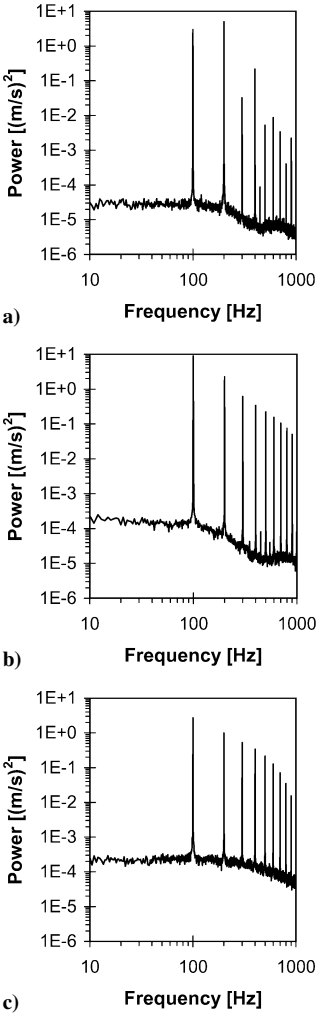

Fig. 6 Frequency spectra of hotwire signal for long-slit cylinder at jet centerline at $Z/h = 0$ for excitation of 100 Hz and 4 V: a) $X/h = 0.67$, b) $X/h = 6.67$, and c) $X/h = 13.33$.

these measurements are not shown. Mean and rms velocity profiles were normalized by the mean centerline velocity of he jet, U_c. Thus, the mean velocity profiles show $U' = U/U_c$, where U' is the normalized velocity and U_c is the mean centerline velocity. The total rms profiles depict $u'_t = u_t/U_c$, where u'_t is the normalized total rms value of the velocity fluctuation, and the rms profiles of the fundamental frequency depicts $u'_f = u_f/U_c$, which is the normalized rms value of the velocity fluctuation at the fundamental frequency f. Phase profiles show the phase difference $\Delta\varphi = \varphi - \varphi_c$ between cross-stream Y positions and the jet centerline, where φ and φ_c are the phase values at the measurement Y position and the jet centerline position, respectively.

All mean velocity profiles collapse when plotted in the usual similarity variables for turbulent jets in accordance with the results of Refs. 7 and 8. The rms profiles show similar trends for both the short- and the long-slit cases; however, the long-slit case shows some scatter. This scatter was observed for other excitation frequencies and amplitude for the long-slit case. The scatter may be attributed to the fact that the wide span of the long slit produces jets with larger spanwise variations in mean velocities and other characteristics as discussed in the following sections. These variations are not present for the more uniform short-slit case, and hence, the profiles collapse better when plotted against similarity coordinates.

Measurements of the spanwise distributions of the centerline characteristics of the issuing jets are discussed in the following sections. These measurements require accurate determination of the mean centerline velocity and phase of the issuing jets as well as the rms amplitudes of the velocity fluctuations. The profiles shown in Figs. 7 and 8 show that the variations in the mean velocity and in the phase angle are very small near the centerline of the jets. In other words, the profiles are flat at the jet centerline. This fact, together with the high accuracy of the traversing mechanism, 0.005 mm/step, provided an adequate measurement procedure to ensure minimal misalignment errors when determining the centerline values of the jet.

B. Effect of Frequency Variation

For this set of experiments, the excitation amplitude was set at 4 V and the excitation frequency was varied between 80, 100, and 120 Hz. The spanwise distributions of the averaged centerline velocity, rms velocity fluctuations, and averaged phase of the velocity fluctuations are shown for the long-slit jet in Fig. 9 and for the short-slit jet in Fig. 10. The phase values in Figs. 9 and 10 are the centerline difference in phase, $\Delta\theta = \varphi_c - \varphi_{cm}$, between each measurement spanwise position and the midspan of the slit, where φ_c and φ_{cm} are the centerline phase values at the measurement spanwise position and the slit midspan, respectively.

For the long-slit case, note in Fig. 9 that the emanating jet is almost symmetric about the midspan position, which was to be expected because the speakers are positioned symmetrically and activated in-phase. Moreover, the mean velocity decreases as we progress toward the midspan of the cylinder from either end. Also, the velocity of the jet decreases and the deficit at the midspan increases with increasing the excitation frequency. The value of the mean velocity at the midspan decreases by about 14% from the value at 80 when switching from 80 to 100 Hz and by about 30% when switching from 80

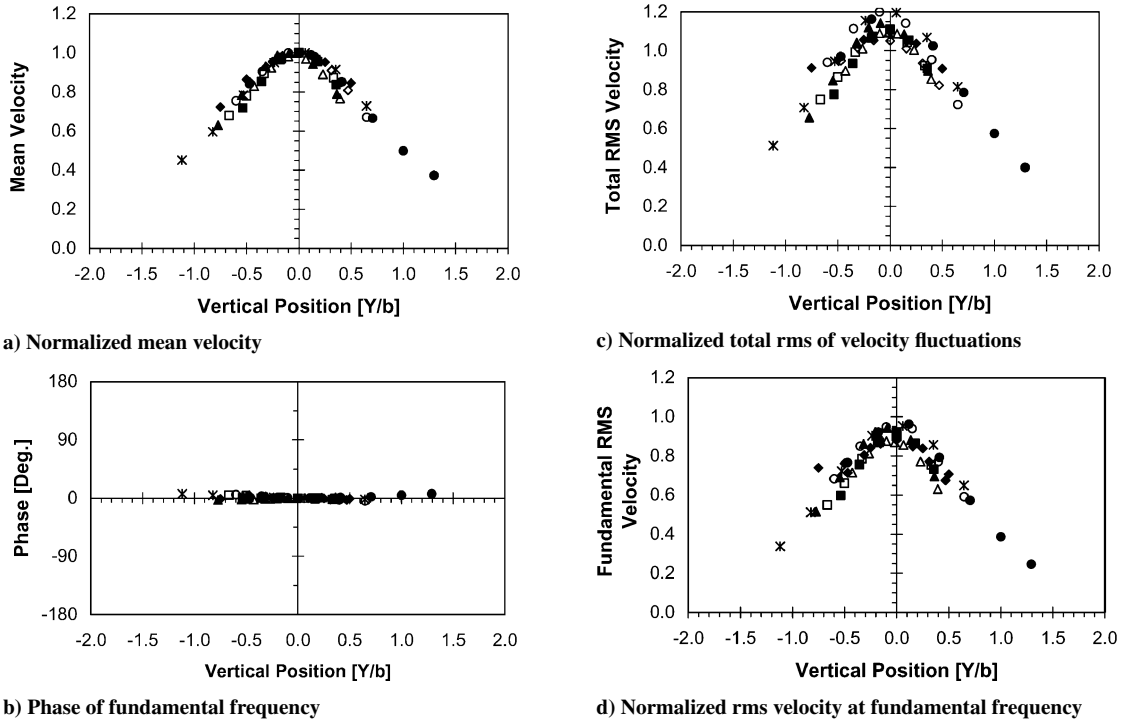

a) Normalized mean velocity

c) Normalized total rms of velocity fluctuations

b) Phase of fundamental frequency

d) Normalized rms velocity at fundamental frequency

Fig. 7 Mean velocity, phase, and rms fluctuation profiles for long slit excited with 80-Hz frequency and 4-V amplitude: Z/h = ♦, −309; ■, −232; ▲, −155; ●, −77; ∗, 0; ○, 77; △, 155; □, 232; and ◇, 309.

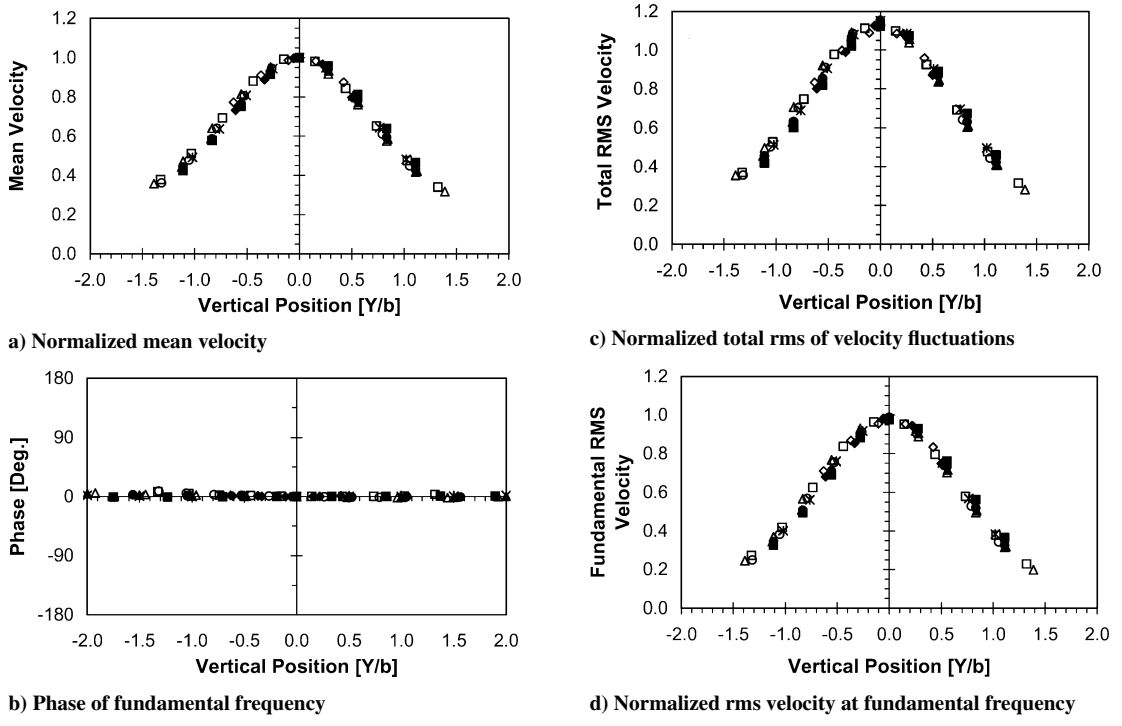

a) Normalized mean velocity

c) Normalized total rms of velocity fluctuations

b) Phase of fundamental frequency

d) Normalized rms velocity at fundamental frequency

Fig. 8 Mean velocity, phase, and rms fluctuation profiles for short slit excited with 80-Hz frequency and 4-V amplitude: Z/h = ♦, −120; ■, −100; ▲, −67; ●, −33; ∗, 0; ○, 33; △, 67; □, 100; and ◇, 120.

to 120 Hz. The deficit at the midspan, on the other hand, increases from about 18% of the velocity at the slit terminations for the 80-Hz case to 28% for the 100-Hz case and to 41% for the 120-Hz case. This same trend exists for the phase change inasmuch as it can be seen that large phase differences occur between the midspan and the ends of the slit. These deficits vary from about 70 deg for the 80-Hz case to about 113 for 120 Hz.

The short-slit case clearly displays a much stronger and more uniform jet. For the same excitation, Fig. 10 shows that the mean centerline velocity of the jet at the midspan increases by an average value of about 79% from the value of the long-slit jet. The jets are more uniform for the short slit, for which the values of the deficit drop to an average value of about 14% in comparison to an average of about 29% for the long-slit case. The phase, as well, is more uniform along the span of the short slit, where the values of the phase difference between the ends of the slit and its midspan drop substantially. Values of phase change for the short-slit cylinder drop to 8 deg for 80 Hz, 11 deg for 100 Hz, and 13 deg for 120 Hz. These

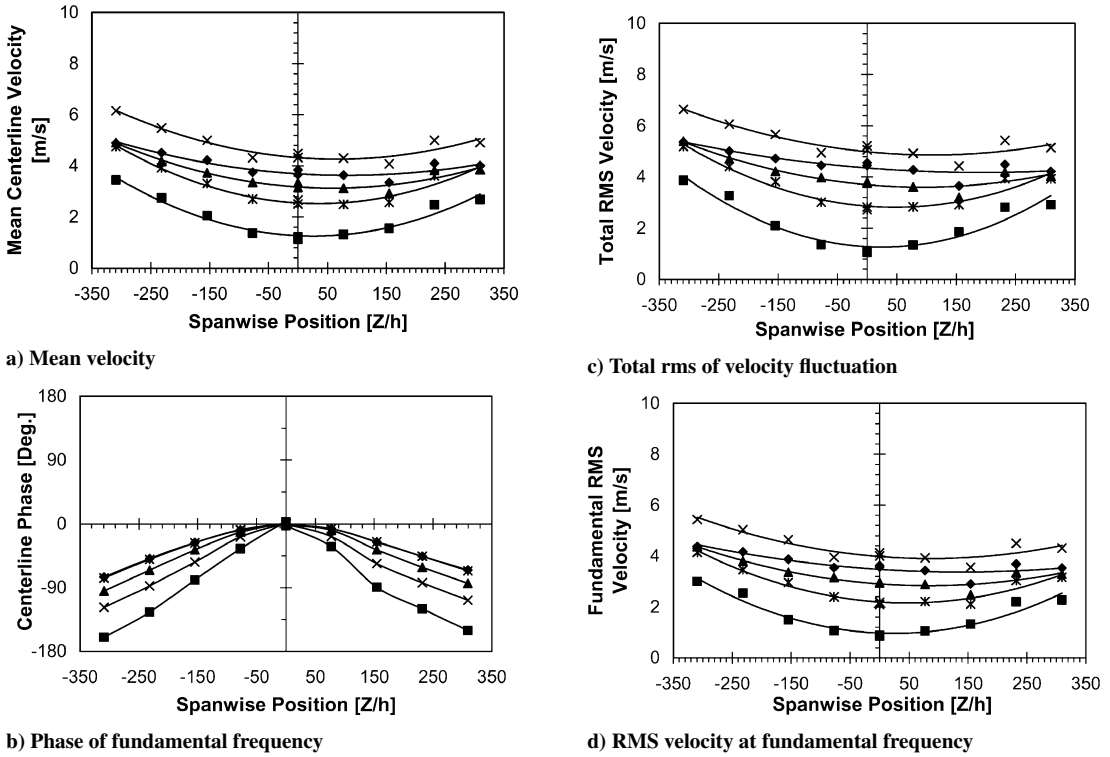

Fig. 9 Spanwise distributions of mean centerline velocity, centerline rms velocity fluctuations, and centerline phase for selected values of excitation frequency and amplitude, long-slit cylinder: ♦, 80 Hz, 4 V; ■, 100 Hz, 2 V; ▲, 100 Hz, 4 V; × , 100 Hz, 6 V; and ∗, 120 Hz, 4 V.

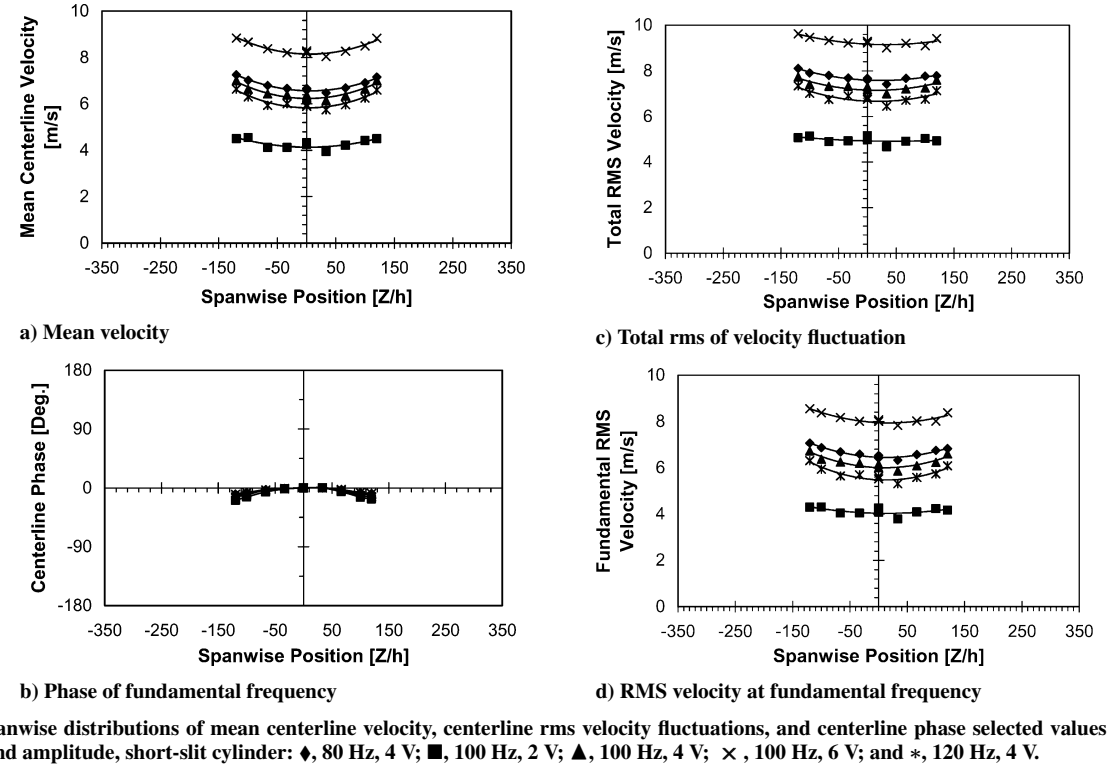

Fig. 10 Spanwise distributions of mean centerline velocity, centerline rms velocity fluctuations, and centerline phase selected values of excitation frequency and amplitude, short-slit cylinder: ♦, 80 Hz, 4 V; ■, 100 Hz, 2 V; ▲, 100 Hz, 4 V; × , 100 Hz, 6 V; and ∗, 120 Hz, 4 V.

are relatively small phase changes along the whole length of the slit. Note, however, that care should be taken when comparing the absolute values of phase because the short and the long slits have different mean velocities, which causes differences in the phase that are induced merely by the differences in the convection velocity.

C. Effect of Amplitude Variation

In this case, the frequency of excitation was fixed at 100 Hz and the amplitude was changed between 2, 4, and 6 V for both slit cases.

Figures 9 and 10 show that, for the case of varying the amplitude of the exciting signal, similar trends, as with varying the frequency, are observed for both the long- and the short-slit cases. All cases show a deficit in both the mean velocity and phase as the midspan of the jet is approached from either end. In this case, however, changing the amplitude produces higher changes in the mean velocity than changing the frequency, but the deficit value stays almost unchanged for different excitation amplitudes.

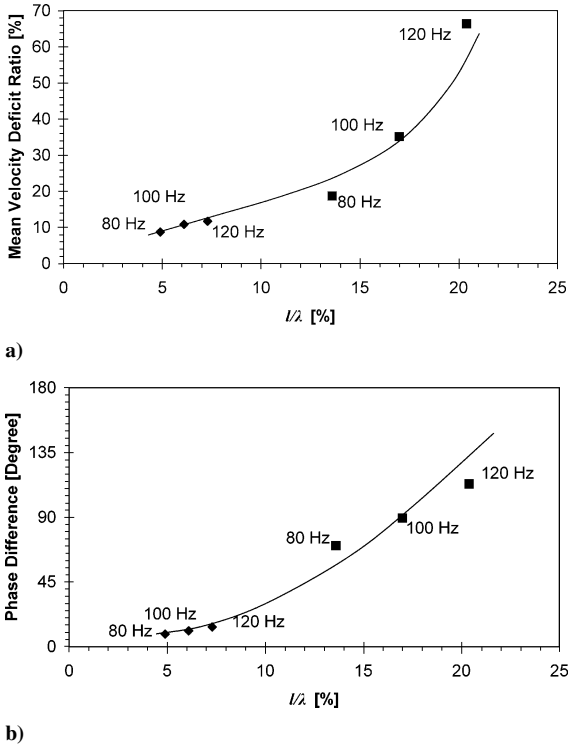

Fig. 11 Effect of wavelength of sound field on a) ratio of spanwise velocity deficit to midspan mean velocity and b) phase difference between cylinder termination and midspan, 4-V excitation amplitude: ♦, short slit and ■, long slit.

The value of the velocity deficit for the long-slit case is about 25% for both the 4- and 6-V excitation, and the value of the phase deficit is about 72 deg. Note, however, that the 2-V case shows a slightly different trend, as will be discussed later.

For the short-slit cylinder, the same behavior exists as mentioned for the long-slit cylinder where the deficit is about 7% for all of the cases and the phase deficit is about 10 deg. The 2-V excitation for the short slit, however, does not show a different behavior than the other two cases.

V. Discussion

The preceding results show that both the amplitude and frequency of excitation have a significant influence on the emanating jet. Moreover, the behavior of the synthetic jet is substantially different for the long-slit case from that of the short-slit one. In general, the short-slit case provided synthetic jets that are stronger and more uniform than those formed for the long-slit case.

The effect of increasing the amplitude of excitation in both the short- and long-slit cases is mainly to increase the velocity of the issuing jet at all spanwise locations. Hence, the deficit in the spanwise distributions of the mean velocity remains almost unchanged when the amplitude is increased. The phase distributions, however, do not show a simple relationship with amplitude because variations in phase caused by different convection velocities of the jet have to be taken into consideration, as well as the nonlinear behavior of the orifices.

The case of the 2-V excitation in the long-slit case shows different trends for the distribution of velocity and phase than the other cases of the long slit. For this case, the deficit in the velocity was 63% as compared to 25% for the other two amplitudes. For the phase, the deficit is about 161 deg for the 2-V case as compared to 72 deg for the other two. Moreover, the trend that the phase distribution follows appears to be different from the other two cases. These changes in the behavior can be attributed to the fact that this amplitude of 2 V represents the lowest excitation level during the tests. It can be expected that, at this low-excitation level, the jet is approaching the formation limit below which the jet is not synthesized.[7,8,14] This supposition is supported by the fact that the changes are more pronounced near the midspan of the long-slit case, where the jet is at its lowest mean velocity.

The excitation frequency variation, on the other hand, produces a change in the deficit of the mean velocity distribution rather than in the magnitude of the jet velocity. This variation can be attributed to a stronger effect on the pressure amplitude inside the cylinder as the frequency of excitation is changed. As the pressure wave, which produces the jet by the pressure difference across the slit, is applied at the cylinder terminations, its amplitude reduces as it travels along the cylinder and its energy is partially dissipated through the slit. As the excitation wavelength is decreased, by increasing the excitation frequency, the cylinder length becomes a larger fraction of the wavelength, which results in larger phase shifts as the sound wave travel along the cylinder. Therefore, the synthetic jet becomes less uniform in amplitude and phase as the ratio between the slit length and wavelength is increased, l/λ. This can be further explained by investigating the effect of the ratio between the slit length and the wavelength of the sound field inside the cylinder, l/λ, on the amplitude ratio and the phase difference between the terminations of the slit and the midspan as shown in Fig. 11. Data corresponding to both the short- and long-slit cases are shown in Fig. 11. It can be seen that, as the l/λ ratio increases, the difference between the magnitude of the jet velocity at the end of the slit and the midspan increases, as well as the phase difference becomes bigger.

The preceding discussion shows that the issue of how long a slit should be to be useful as a control actuator is rather application dependent. The optimal slit length depends on how uniform a synthetic jet is required to be, as well as on the geometrical and operational parameters of the actuator, which dictates the dimensions of the slit and the range of frequencies of interest. Longer slits require lower frequencies to maintain the uniformity of the jet, whereas shorter slits can produce uniform jets at higher frequencies.

VI. Conclusions

The characteristics of two synthetic jets with high aspect ratios are investigated experimentally. The jets are produced through axial slits on the surfaces of two cylinders and are excited acoustically by a pair of speakers mounted on the cylinder terminations. The main objective of the experiments is to investigate the spanwise characteristics of the synthetic jets for the prospect of their use as actuators for active flow control. The characteristics of interest are the spanwise distribution of the averaged mean centerline velocity and the amplitude and phase distributions of velocity fluctuations at the jet centerline.

First, the characteristics of the issuing jet at different spanwise locations were investigated. Transverse profiles of mean and fluctuating velocity and phase distributions were found to agree well with those reported in the literature for synthetic jets. The effects of varying the amplitude and frequency of the loudspeaker excitation on the spanwise characteristics of the jet were then studied. It was found that the nonuniform excitation causes the jet characteristics to vary along the span of the slit. The large differences between the characteristics of the jet in the long-slit and the short-slit cases can be related to the much larger values of l/λ for the long-slit case. These large values of l/λ indicate that the slit length constitutes a substantial part of the wavelength of the sound field inside the cylinder cavity, thereby, introducing larger variations in the magnitude and phase of the issuing jet. At the midspan of the cylinder, deficits in the mean centerline velocity of the jet were as high as 40% for the long-slit case, but were much smaller, about 10%, for the short-slit case. Similar dependence on the spanwise position was observed for both the rms fluctuations and the phase distribution. Phase deficits up to 113 deg for the long slit and 13 deg for the short slit were recorded. The short slit, in general, produced a stronger and more uniform jet than that generated by the long slit under similar excitation conditions.

It can be concluded that synthetic jets issuing from slits on the surface of cylinders and generated by loudspeakers attached to the cylinder terminations can display large spanwise variations in their properties. These variations are rather substantial if the ratio of l/λ

is larger than 8%. In the present tests, for example, the short slit produced virtually uniform jets for $l/\lambda < 8\%$, despite its relatively high aspect ratio, $l/h = 273$. This uniform synthetic jet is a more favorable actuator for active flow control applications because small phase variations of the jet are a desirable attribute of a control actuator. On the other hand, the long-slit jet studied here could be useful for open-loop control applications, in which the inducement of large phase variations along the slit is likely to produce beneficial effects. For example, it may be used to preclude the synchronization of vortex shedding from the cylinder.

References

[1]Ingrad, U., and Labate, S., "Acoustic Circulation Effects and the Nonlinear Impedance of Orifices," *Journal of the Acoustic Society of America*, Vol. 22, No. 2, 1950, pp. 211–218.

[2]Smith, B. L., and Glezer, A., "Vectoring of a High Aspect Ratio Rectangular Air Jet Using a Zero-Net-Mass-Flux Control Jet," *Bulletin of the American Physical Society*, Vol. 39, 1994, p. 1894.

[3]Ziada, S., "Feedback Control of Globally Unstable Flows: Impinging Shear Flows," *Journal of Fluids and Structures*, Vol. 9, No. 8, 1995, pp. 907–923.

[4]Lebedeva, I. V., "Experimental Study of Acoustic Streaming in the Vicinity of Orifices," *Soviet Physics Acoustics*, Vol. 26, No. 4, 1980, pp. 331–333.

[5]Ziada, S., "Feedback Control of Global Flow Oscillations," *Engineering Mechanics*, Vol. 6, No. 4/5, 1999, pp. 337–354.

[6]McCormick, D. C., "Boundary Layer Separation Control with Directed Synthetic Jets," AIAA Paper 2000-0519, Jan. 2000.

[7]Smith, B. L., and Swift, G. W., "Synthetic Jets at Large Reynolds Number and Comparison to Continuous Jets," AIAA Paper 2001-3030, June 2001.

[8]Smith, B. L., and Swift, G. W., "A Comparison Between Synthetic Jets and Continuous Jets," *Experiments in Fluids*, Vol. 34, No. 4, 2003, pp. 467–472.

[9]Wolfe, D., and Ziada, S., "Feedback Control of Vortex Shedding from Two Tandem Cylinders," *Journal of Fluids and Structures*, Vol. 17, No. 4, 2003, pp. 579–592.

[10]Smith, B. L., and Glezer, A., "Vectoring and Small-Scale Motions Effected in Free Shear Flows Using Synthetic Jet Actuators," AIAA Paper 97-0213, 1997.

[11]Smith, B. L., and Glezer, A., "The Formation and Evolution of Synthetic Jets," *Physics of Fluids*, Vol. 10, No. 9, 1998, pp. 2281–2297.

[12]Mallinson, S. G., Reizes, J. A., and Buttini, M., "Synthetic Jets for Flow Control," *Proceedings of the SPIE Asia/Pacific Symposium on Microelectronics and MEMS*, Vol. 3891, Society of Photo-Optical Instrumentation Engineers (International Society for Optical Engineering), Bellingham, WA, 1999, pp. 146–156.

[13]Gilarranz, J. L., and Rediniotis, O. K., "Compact, High-Power Synthetic Jet Actuators for Flow Separation Control," AIAA Paper 2001-0737, Jan. 2001.

[14]Utturkar, Y., Holman, R., Mittal, R., Carroll, B., Sheplak, M., and Cattafesta, L., "A Jet Formation Criterion for Synthetic Jet Actuators," AIAA Paper 2003-0636, Jan. 2003.

[15]Utturkar, Y., Mittal, R., Rampunggoon, P., and Cattafesta, L., "Sensitivity of Synthetic Jets to the Design of the Jet Cavity," AIAA Paper 2002-0124, Jan. 2002.

[16]Gallas, Q., Holman, R., Nishida, T., Carroll, B., Sheplak, M., and Cattafesta, L., "Lumped Element Modeling of Piezoelectric-Driven Synthetic Jet Actuators," *AIAA Journal*, Vol. 41, No. 2, 2003, pp. 240–247.

[17]Gallas, Q., Wang, G., Papila, M., Sheplak, M., and Cattafesta, L., "Optimization of Synthetic Jet Actuators," AIAA Paper 2003-0635, Jan. 2003.

[18]Rediniotis, O. K., Ko, J., Yue, X., and Kurdila, A. J., "Synthetic Jets, Their Reduced-Order Flow Modeling and Applications to Flow Control," AIAA Paper 99-1000, Jan. 1999.

[19]Crook, A., and Wood, N. J., "Measurements and Visualizations of Synthetic Jets," AIAA Paper 2001-0145, Jan. 2001.

[20]Ziada, S., "Control of Fluid–Structure–Sound Interaction Mechanisms by Means of Synthetic Jets," *JSME International Journal, Series C*, Vol. 46, No. 3, 2003, pp. 873–880.

[21]Hsiao, F., and Shyu, J., "Influence of Internal Acoustic Excitation upon Flow Passing a Circular Cylinder," *Journal of Fluids and Structures*, Vol. 5, No. 4, 1991, pp. 427–442.

[22]Huang, X. Y., "Suppression of Vortex Shedding from a Circular Cylinder by Internal Acoustic Excitation," *Journal of Fluids and Structures*, Vol. 9, No. 5, 1995, pp. 563–570.

[23]Miller, R. M., and Tunkel, R. N., "Vibration-Driven Acoustic Jet Controlling Boundary Layer Separation," U.S. Patent 6,109,566, 29 Aug. 2000.

[24]Mittal, R., Rampunggoon, P., and Udaykumar, H. S., "Interaction of a Synthetic Jet with a Plate Boundary Layer," AIAA Paper 2001-2773, June 2001.

[25]Amitay, M., Honohan, A. M., Trautman, M., and Glezer, A., "Modification of the Aerodynamic Characteristics of Bluff Bodies Using Fluidic Actuators," AIAA Paper 97-2004, June–July 1997.

[26]Smith, D. R., Amitay, M., Kibens, V., Parekh, D. E., and Glezer, A., "Modification of Lifting Body Aerodynamics Using Synthetic Jet Actuators," AIAA Paper 98-0209, Jan. 1998.

[27]Glezer, A., Smith, B. L., and Trautman, M. A., "Modifications of Fluid Flow About Bodies and Surfaces with Synthetic Jet Actuators," U.S. Patent 5,957,413, 28 Sept. 1999.

[28]Mittal, R., and Rampunggoon, P., "Brief Communications: On the Virtual Aeroshaping Effect of Synthetic Jets," *Physics of Fluids*, Vol. 14, No. 4, 2002, pp. 1533–1536.

[29]Glezer, A., and Smith, B. L., "Synthetic Jet Actuators for Modifying the Direction of Fluid Flows," U.S. Patent 5,988,522, 23 Nov. 1999.

[30]Smith, B. L., and Glezer, A., "Jet Vectoring Using Synthetic Jets," *Journal of Fluid Mechanics*, Vol. 458, 2002, pp. 1–34.

[31]Glezer, A., Allen, M. G., Coe, D. J., Smith, B. L., Trautman, M. A., and Wiltse, J. W., "Synthetic Jet Actuators and Applications Thereof," U.S. Patent 5,758,823, 2 June 1998.

[32]Glezer, A., Allen, M. G., Coe, D. J., Smith, B. L., Trautman, M. A., and Wiltse, J. W., "Synthetic Jet Actuators and Applications Thereof," U.S. Patent 5,894,990, 20 April 1999.

[33]Davis, S. A., and Glezer, A., "Mixing Control of Fuel Jets Using Synthetic Jet Technology," AIAA Paper 99-0447, Jan. 1999.

[34]Glezer, A., and Wiltse, J. W., "Synthetic Jet Actuators for Mixing Applications," U.S. Patent 6,056,204, 2 May 2000.

[35]Glezer, A., and Amitay, M., "Synthetic Jets," *Annual Review of Fluid Mechanics*, Vol. 34, 2002, pp. 503–529.

S. Aggarwal
Associate Editor